DOI: 10.1002/chem.200700649

Structural Importance of Secondary Interactions in Molecules: Origin of Unconventional Conformations of Phosphine–Borane Adducts

Patrick Spies, Roland Fröhlich, Gerald Kehr, Gerhard Erker,* and Stefan Grimme*[a]

Dedicated to Professor Hans J. Schäfer on the occasion of his 70th birthday

Abstract: The series of phosphine–borane adducts, $Ph_2(H_3C{-}C{\equiv}C)P{-}B(C_6F_5)_3$ (**8c**), $Ph(H_3C{-}C{\equiv}C)_2P{-}B(C_6F_5)_3$ (**8b**) and $(H_3C{-}C{\equiv}C)_3P{-}B(C_6F_5)_3$ (**8a**), was prepared. The X-ray crystal structure analyses revealed close to eclipsed conformations for all members of this series with average dihedral angles θ(C-P-B-C) of 8.1° (**8c**), 12.3° (**8b**) and 20.3° (**8a**). Quantum chemical analysis of these compounds revealed the importance of a subtle interplay between competing attractive and repulsive secondary interactions, causing the surprising eclipsed conformational preference for systems of this degree of complexity. Some cyclic phosphine–borane adducts were studied for comparison.

Keywords: boranes · donor–acceptor systems · phosphines · quantum chemical calculations · structure elucidation

Introduction

Most saturated hydrocarbons favour staggered conformations (**A**) substantially over their eclipsed ones (**B**).[1] The latter are usually not even local minimum structures, but rather they represent the transition-state geometries that are passed upon the transition from one stable conformational minimum structure to another. The nature of the energy barrier (and hence the origin of the **A**/**B** energy difference) of the parent hydrocarbon ethane has been (and probably still is) a matter of controversial discussion.[2] For the higher alkanes or systems with spatially (sterically) more demanding substituents it seems commonly accepted that four-electron Pauli repulsion between in-plane C–C σ-bonds make the eclipsed conformer **B** unfavourable. However, recently there has been lively scientific discussion about the fundamental physical and chemical aspects of this interaction and bonding concepts in general, as exemplified for the case of the C–C bond rotation in biphenyl.[3]

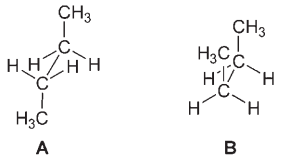

A

B

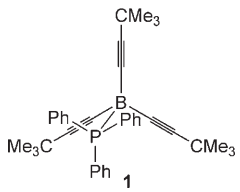

1

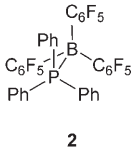

2

One must realise that the overall situation of predicting and understanding the preferred (conformational) structures of molecules often becomes complicated by the interplay of various types of secondary interactions between adjacent subunits. In such situations energetic compensation effects may lead to the observation of unusual or unexpected structural global minima, the appearance of which cannot be rationalised by any simplified general analysis.

The hetero-analogues of the alkanes are prominent examples of such a situation. Examples of both conformers **A** and **B** were experimentally observed for differently substituted borane-phosphine adducts $R_3P{-}BR'_3$.[4,5] The $Ph_3P{-}B(C_6F_5)_3$ system (**2**)[5] is a typical example of an eclipsed structure in the solid state, whereas the related $Ph_3P{-}B(C{\equiv}C{-}CMe_3)_3$ adduct (**1**)[4] exhibits a staggered conformation in the crystal. We synthesised a series of P–B addition products that conceptually may be thought to be located be-

[a] P. Spies, Dr. R. Fröhlich, Dr. G. Kehr, Prof. G. Erker, Prof. S. Grimme
Organisch-Chemisches Institut, Universität Münster
Corrensstr. 40, 48149 Münster (Germany)
Fax: (+49) 251-83-36503
E-mail: erker@uni-muenster.de
gimmes@uni-muenster.de

tween the extremes **1** and **2**, namely the $B(C_6F_5)_3$ adducts of $P(C{\equiv}C{-}CH_3)_3$, $PhP(C{\equiv}C{-}CH_3)_2$ and $Ph_2P(C{\equiv}C{-}CH_3)$. The preferred conformational structures of these heteroanalogues of **A** and **B** in the crystal were determined by X-ray diffraction. The observed structures were then analysed by quantum chemical calculations to reveal the major secondary interaction effects that were responsible for the occurrence of such favoured structural types. This revealed some general features that need to be taken into account to understand or predict the correct structures of more complex "alkane-like" molecular systems. We will begin our discussion with a description of the structural features of a small series of selected cyclic phosphine–borane adducts.

Results and Discussion

Syntheses and structural features of cyclic phosphine–borane adducts: Allylbis(*tert*-butyl)phosphine (**4a**) was synthesised by treatment of chlorobis(*tert*-butyl)phosphine (**3a**) with allylmagnesium bromide.[6a] Subsequent reaction of **4a** with "Piers' borane" $[HB(C_6F_5)_2]$[6b] in toluene at reflux temperatures resulted in a clean hydroboration reaction to yield **5a** (28%) (Scheme 1). Compound **5a** features a single

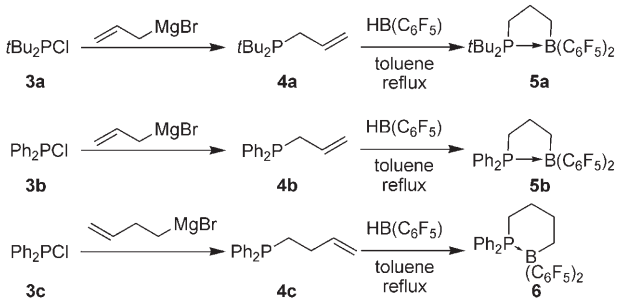

Scheme 1.

^{1}H NMR *tert*-butyl resonance at $\delta = 1.25$ ppm (18H), a broad ^{31}P NMR signal at $\delta = +42$ ppm ($\nu_{1/2} = 140$ Hz) and a typical ^{11}B NMR resonance for a four-coordinated boron atom at $\delta = -10$ ppm. A set of three ^{19}F NMR signals was observed at $\delta = -128.5$ (4F, *o*-), -159.5 (2F, *p*-) and -165.0 ppm (4F, *m*-C_6F_5). The reaction of chlorodiphenylphosphine (**3b**) with the allyl Grignard reagent followed by hydroboration with $HB(C_6F_5)_2$ proceeded similarly to give the five-membered P,B-compound **5b** [51% isolated, ^{13}C NMR of the P-$(CH_2)_3$-B unit at $\delta = 27.2$ (^1J(P,C) = 42.6 Hz), 25.6 (^2J(P,C) = 14.8 Hz), 23.7 ppm (br)]. Compound **5b** featured very typical NMR signals at $\delta = 22.6$ (^{31}P); -9 (^{11}B) and -129.5 (*o*), -158.5 (*p*) and -164.2 ppm (*m*) (^{19}F).

Single crystals were obtained for both **5a** and **5b** (from diethyl ether). Both compounds in the crystal feature five-membered heterocyclic structures, as expected, created by internal adduct formation between the phosphine moieties and the strong Lewis acid boron centres (d(P1–B1) = 2.064(2) (**5a**), 2.060(2) Å (**5b**)). Both compounds exhibit distorted envelope-shaped conformations of the boraphosphacyclopentane core, but they are distinctly different from each other. Compound **5a** shows a conventional envelope conformation with the tBu$_2$P group adjacent to phosphorus atom, representing the tip, and the C1-C2-C3-B1 moiety the almost coplanar base. This leads to an arrangement of the bulky substituents at P and B that is as close as possible to a sterically favourable staggered orientation of the five-membered heterocyclic framework (dihedral angles θ: C8-P1-B1-C21 28.6(1), C8-P1-B1-C31 $-96.5(1)$, C4-P1-B1-C31 47.7(1), C4-P1-B1-C21 172.7(1)°) (Figure 1).

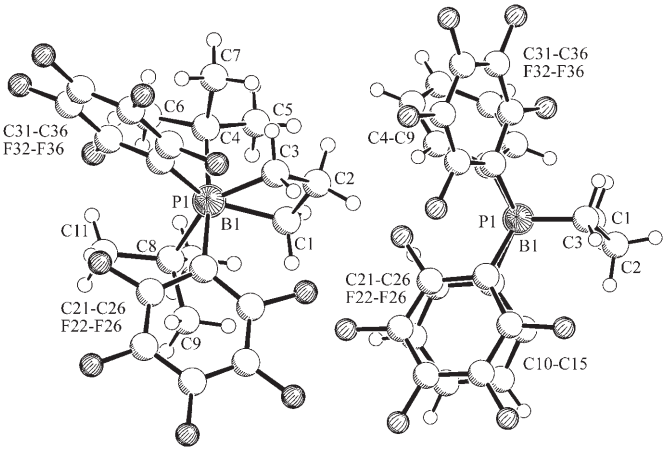

Figure 1. Views of the different envelope type structures of **5a** (left) and **5b** (right).

Compound **5b** also features a distorted envelope conformation in the crystal, but it is distinctly different from **5a** (see Figure 1). In **5b** the central $-CH_2-$ group forms the tip of the envelope and C1-P1-B1-C2 forms the base. This leads to an eclipsed conformational arrangement of the bulky aryl substituents at the adjacent phosphorus and boron centres (dihedral angles θ: C10-P1-B1-C21 $-6.8(1)$, C4-P1-B1-C31 $-4.0(2)$, C10-P1-B1-C31 $-131.9(1)$, C4-P1-B1-C21 121.1(1)°). It may be that this unconventional conformation has become slightly favoured by some π-stacking interaction of the C_6H_5 ring at phosphorus with the C_6F_5 ring at boron. Such π–π arene interactions can be energetically quite substantial, especially when strong acceptors such as the pentafluorophenyl moiety are involved.[7] We note that the C10–C15 phenyl group at P1 and the C21–C26 pentafluorophenyl group at B1 are oriented close to parallel with the framework (angle between the C10–C15 and C21–C26 planes: -24.8°, C21···C10 separation: 3.093 Å).

The corresponding cyclic six-membered P–B adduct **6** was prepared by treatment of Ph_2PCl (**3c**) with butenylmagnesium bromide to yield **4c** (59%) followed by the hydroboration reaction with $HB(C_6F_5)_2$ (see Scheme 1). Compound **6** was isolated in 66% yield as a white solid (^{31}P NMR: $\delta =$ 0.5, ^{11}B NMR: $\delta = -12$ ppm). It features a set of four ^{13}C NMR methylene signals (C1–C4) at $\delta = 23.5$ (^1J(P,C) =

32.2 Hz), 25.5 (^2J(P,C) = 3.6 Hz), 24.6 (^3J(P,C) = 7.7 Hz) and 19.6 ppm (br). Compound **6** exhibits dynamic NMR spectra. At 300 K in [D_2]dichloromethane a sharp ^{19}F NMR signal at $\delta = -163.0$ ppm (*m*-C_6F_5), a slightly broadened *p*-C_6F_5 resonance at $\delta = -157.8$ ppm, and a very broad *o*-C_6F_5 signal at $\delta = -128.4$ ppm were observed. Upon lowering the monitoring temperature (see Figure 2) the *p*-C_6F_5 resonance rapidly

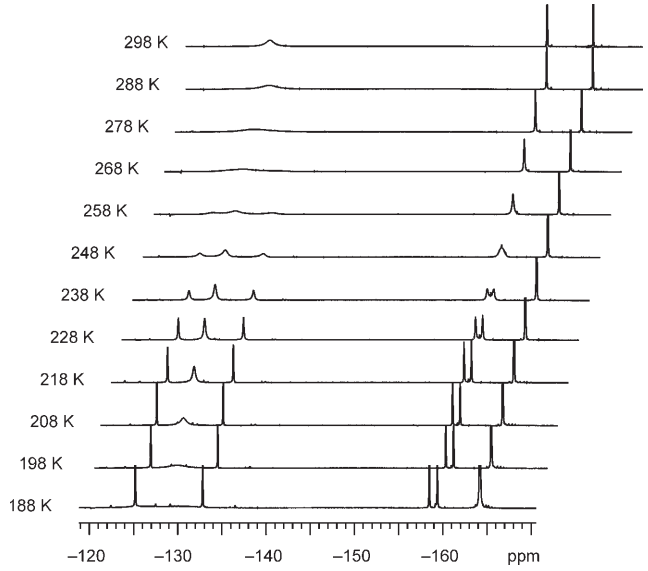

Figure 2. Temperature dependent ^{19}F DNMR spectra of **6** ([D_2]dichloromethane, 564 MHz).

splits into a 1:1 pair of signals, whereas the *o*-C_6F_5 signals decoalesces into a sharp 1:1 pair and a broad signal, each of relative intensity 2. The *m*-C_6F_5 resonances of the system are isochronous and do not change much with temperature.

The characteristic appearance of the temperature-dependent ^{19}F NMR signals of **6** indicates "freezing" of the inversion process of the conventional cyclohexane chair framework (see below) with decreasing temperature, which leads to a differentiation between axial and equatorial $-C_6F_5$ substituents, in addition to an increasingly hindered rotation around the B$-C_6F_5$ vectors.[8] From the coalescence behaviour we estimated a Gibbs activation energy of $\Delta G^{\ddagger}_{inv}(243\ K) = 10.7 \pm 0.5$ kcal mol^{-1} for the ring inversion process and $\Delta G^{\ddagger}_{rot}(275\ K) = 11.0 \pm 0.5$ kcal mol^{-1} for the rotation barrier of the first B$-C_6F_5$ unit (the second value could not be obtained from this experiment, see Figure 2).

Single crystals of **6** suitable for X-ray crystal structure analysis (see Figure 3) were obtained from diethyl ether. The crystal features four-coordinate pseudotetrahedral boron and phosphorus centres (d(P1–B1) = 2.021(3) Å). Compound **6** exhibits a close to ideal chair conformation with a nearly perfect staggering of the bulky aryl substituents along the P–B vector (see the respective projection in Figure 3, left). The corresponding dihedral angle of the antiperiplanar substituents amounts to C21-P1-B1-C31: −179.6(2)°, the respective gauche orientations are characterised by dihedral angles C11-P1-B1-C41 −60.9(2), C11-P1-B1-C31 57.9(2), C21-P1-B1-C41 61.6(2) and C1-P1-B1-C4 49.8(2)°.

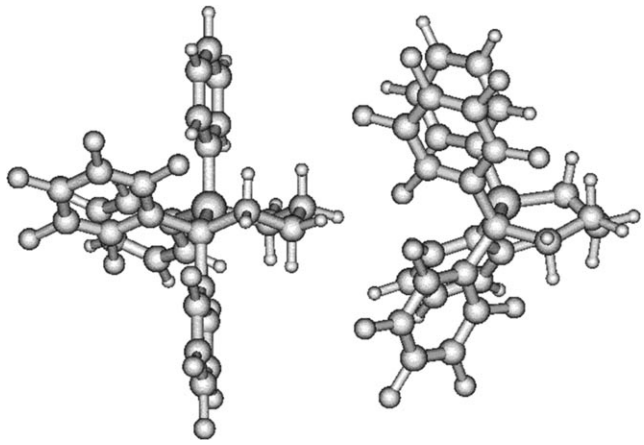

Figure 3. Views of the conformational arrangements of the experimentally determined global minimum chair structure (left) and a DFT calculated local minimum twist structure of **6** (right).

A DFT calculation also finds a respective conventional chair conformation as the global minimum; only the C_6H_5 and C_6F_5 groups are slightly rotated in the gas-phase calculation. However, the DFT calculation located a second conformer as a local minimum, energetically only 1.7 kcal mol^{-1} less favourable than the global minimum chair conformer. This isomer exhibits a distorted twist-conformation. It is characterised by an eclipsed geometric arrangement of the substituents along the P–B vector. The negative influence by steric hindrance in this unconventional arrangement is apparently more than compensated by some positive arene π–π interaction between the coplanar C_6H_5/C_6F_5 pair at the P–B unit (see Figure 3, right).

So far this study has shown that the favoured structures of bulky phosphine–borane adducts may be influenced by a variety of stabilizing and destabilizing forces, which may make them difficult to predict. We therefore studied a related series of acyclic phosphine–borane adducts in some detail, all of which have favoured unconventional conformational structures.

Syntheses and spectroscopic characterisation of new phosphine–B(C_6F_5)$_3$ adducts: The phosphines used for this study were prepared analogously to published procedures (Scheme 2). Thus, treatment of Ph_2PCl with one molar equivalent of propynyllithium gave $Ph_2P(C{\equiv}C{-}CH_3)$ (**7c**).[9] The compound features a typical ^{31}P NMR resonance at $\delta = -32.0$ ppm and a sharp $\tilde{\nu}$(C≡C) IR band at 2183 cm^{-1}. Similarly, treatment of the related starting material $PhPCl_2$ with two molar equivalents of the Li$-$C≡C$-CH_3$ reagent yielded $PhP(C{\equiv}C{-}CH_3)_2$ (**7b**)[10] (^{31}P NMR $\delta = -43.0$ ppm, IR: $\tilde{\nu} = 2182$ cm^{-1}), and three equivalents propynyllithium were treated with PCl_3 to yield $P(C{\equiv}C{-}CH_3)_3$ (**7a**)[11] (^{31}P NMR $\delta = -86.3$ ppm, IR: $\tilde{\nu} = 2189$ cm^{-1}].

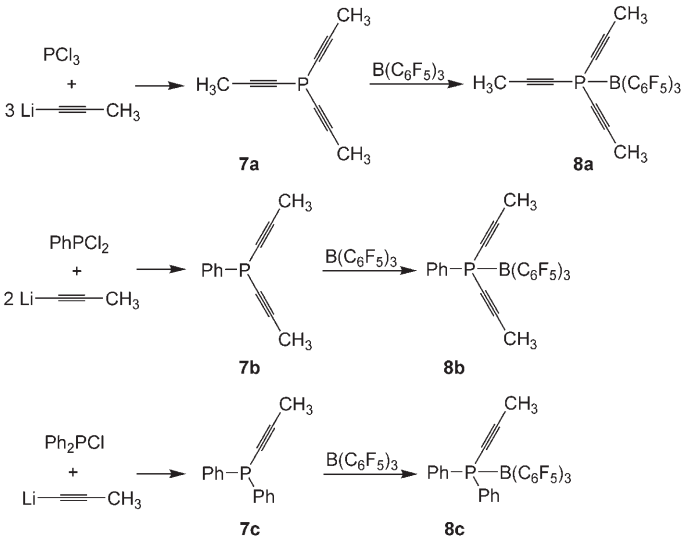

Scheme 2.

The reaction of **7c** with $B(C_6F_5)_3$ was carried out at ambient temperature in toluene. The usual workup (for details see the Experimental Section) gave the adduct (**8c**) as a white solid in 78% yield. The $PhP(C{\equiv}C{-}CH_3)_2/B(C_6F_5)_3$ adduct (**8b**) was prepared from the phosphine **7b** and tris(pentafluorophenyl)borane (54% isolated). Compound **8c** features a ^{31}P NMR resonance at $\delta = 6.4$ ppm. The ^{11}B NMR signal of **8c** is observed at $\delta = -8$ ppm (cf. free $B(C_6F_5)_3$: $\delta = 60$ ppm[12]). The $Ph(H_3C{-}C{\equiv}C)_2P{-}B(C_6F_5)_3$ adduct (**8b**) features a ^{31}P NMR resonance at $\delta = -15$ ppm. The coordinated $B(C_6F_5)_3$ unit shows NMR data that is quite different from the free tris(pentafluorophenyl)borane Lewis acid. It features a set of three ^{19}F NMR multiplets at $\delta = -127.3$ (*o*), -157.2 (*p*) and -165.3 ppm (*m*). Free $B(C_6F_5)_3$ characteristically shows a much wider separation of the respective *p*-F and *m*-F resonances (free $B(C_6F_5)_3$: $\delta = -129.1$ (*o*), -142.4 (*p*), -160.3 ppm (*m*)).[12] The ^{11}B NMR resonance of compound **8b** is found at $\delta = -7$ ppm. The adduct **8b** features a sharp alkynyl IR band at 2204 cm^{-1}. Tris(pentafluorophenyl)borane was treated with tripropynylphosphine (**7a**) in toluene at ambient temperature to give the 1:1 adduct (**8a**) in 63% yield. It shows the typical NMR features of both a tetra-coordinated phosphorus atom (^{31}P NMR: $\delta = -38.0$ ppm) and a tetra-coordinated boron (^{11}B NMR: $\delta = -9$ ppm). The ^{19}F NMR spectrum shows a typical set of corresponding C_6F_5 resonances at $\delta = -126.0$ (*o*), -155.2 (*p*) and -163.2 ppm (*m*-C_6F_5). The ^{13}C NMR signals of the $P(C{\equiv}C{-}CH_3)_3$ substituent were found at $\delta = 108.9$ ($^2J(P,C) = 25.6$ Hz, β-C), 64.1 ($^1J(P,C) = 156.8$ Hz, α-C) and 5.2 ppm ($^3J(P,C) = 3.5$ Hz, CH_3).

X-ray crystal structure analyses of the adducts: The structures of all three $B(C_6F_5)_3$-phosphine adducts (**8a–c**) were determined by X-ray diffraction.[13–15] Single crystals of **8c** that were suited for the X-ray crystal structure determination were obtained from diethyl ether. The structure (Figure 4) shows that a new phosphorus–boron bond was formed (P–B: 2.157(3) Å). Although this P–B linkage is rather long, bond formation between the group 13 and

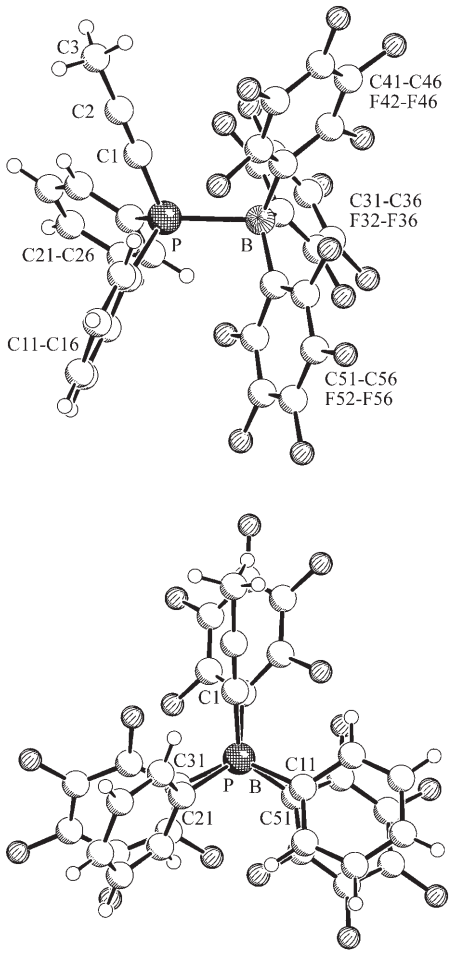

Figure 4. Two views of the molecular structure of **8c**.

group 15 element results in a severe distortion of the remaining bond angles at both the main group element centres upon going from the three- to four-coordinate states. With respect to the free phosphine all distal C-P-C angles at phosphorus have opened up to approximately 104° upon adduct formation (C1-P-C21 104.1(2), C1-P-C11 104.6(1), C11-P-C21 104.2(2)°). The bond angles at phosphorus which are proximal to the boron centre are much larger at 110.3(2) (C1-P-B), 114.4(1) (C11-P-B), and 118.0(1)° (C21-P-B). The P–C1 bond (1.718(4) Å) is much shorter than the adjacent P–arene σ-bonds (P–C11 1.823(3), P–C21 1.823(3) Å). The C1–C2 bond is in the typical range of a C≡C triple bond (1.204(4) Å)[13] and the adjacent (sp)C2–(sp^3)C3 bond amounts to a typical 1.461(5) Å. The three B–C carbon σ-bonds to the C_6F_5 rings were found in a very close range between 1.628(5) and 1.636(5) Å. The distal C–B–C angles are found to be 111.0(3) (C31-B-C41), 114.0(3) (C41-B-C51) and 115.6(3)° (C31-B-C51). All three are larger than the proximal angles (C31-B-P 102.7(2), C51-B-P 103.5(2), C41-

B-P 108.9(2)°). The conformation of the six substituents at the P–B unit in compound **8c** is eclipsed. Typical dihedral angles θ that characterise this situation are, for example, C11-P-B-C51: 10.2(2), C21-P-B-C31: 7.8(3) and C1-P-B-C41: 6.2(3)°.

Compound **8b** shows similar structural features in the crystal (Figure 5). As compared to **8c** the P–B bond in **8b** seems to be marginally stronger, as judged from its slightly

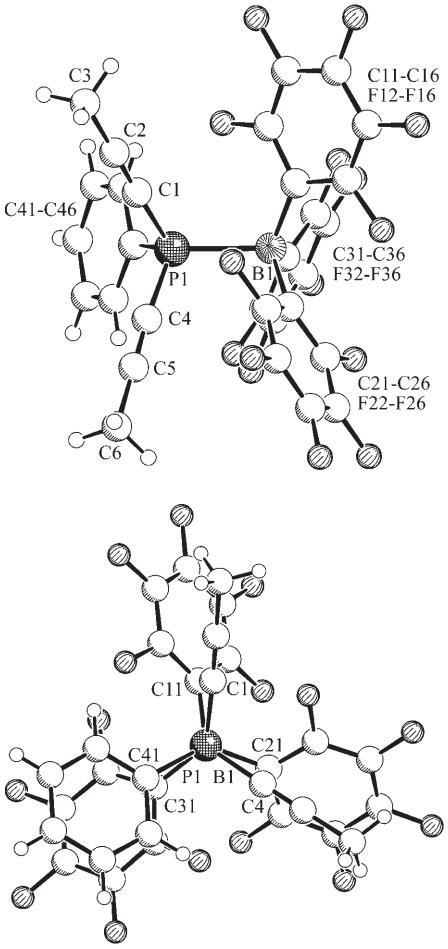

Figure 5. Two views of the molecular structure of **8b**.

shorter length (**8b**; P1–B1: 2.125(2) Å). The overall conformation in **8b** is again eclipsed with pertinent dihedral angles θ being for example, −13.9(1) (C4-P1-B1-C21), −12.8(2) (C1-P1-B1-C11) and −10.1(1)° (C41-P1-B1-C31). The P–acetylide bond lengths again are short (P1–C1 1.741(2), P1–C4 1.740(2) Å) as compared to the remaining P–arene linkage (P1–C41 1.813(2) Å). The bond angles at P1 fall into two groups: being within a narrow range between 104.2(1) and 105.6(1)° on the "distal" side, and amounting to larger values of 109.3(1) (C4-P1-B1), 115.6(1) (C41-P1-B1) and 116.3(1)° (C1-P1-B1) in the "proximal" sector. Conversely, the "proximal" bond angles at B1 are smaller (102.3(1) (C21-B1-P1), 102.6(1) (C31-B1-P1), 108.7(1)° (C11-B1-P1)) than the "distal" angles at the borane end of adduct **8b** (110.8(2) (C11-B1-C21), 114.7(2) (C11-B1-C31), 116.3(2)° (C21-B1-C31)).

Single crystals of the adduct **8a** were obtained from diethyl ether. As expected for a compound derived from the sterically least encumbered phosphine in this series the P–B bond in **8a** (2.062(3) Å) is the shortest of the three adducts. In the crystal the molecule is C_3-symmetric along the P–B vector. Again the *ipso*-$C_{(C6F5)}$-P-B angles (C11-B-P1 105.3(1)°) are markedly smaller than the acetylide-C-P-B angles (C1-P1-B 113.6(1)°). Consequently, the "distal" angles at boron (C11-B-C11* 113.3(1)°) increase and the respective C1-P1-C1′ angles are decreased (105.1(1)°). The P1–acetylide moieties are close to linear (P angles P1-C1-C2 176.9(2), C1-C2-C3 178.0(2)°; bond lengths P1–C1: 1.737(2), C1–C2 1.190(2), C2–C3: 1.463(3) Å). The B–C_6F_5 linkage amounts to B1–C11: 1.633(2) Å.

The $(H_3C–C\equiv C)_3P–B(C_6F_5)_3$ adduct **8a** again exhibits an eclipsed conformation of the substituents at boron and phosphorous along the P–B vector (see Figure 6), although this is the example in this series of adducts that features the largest deviation from the ideal geometric situation. The corresponding dihedral angle θ (C1-P1-B1-C11) was found to be 20.3°(1).

Quantum chemical calculations: To get more insight into the origin of structural preferences for eclipsed or staggered

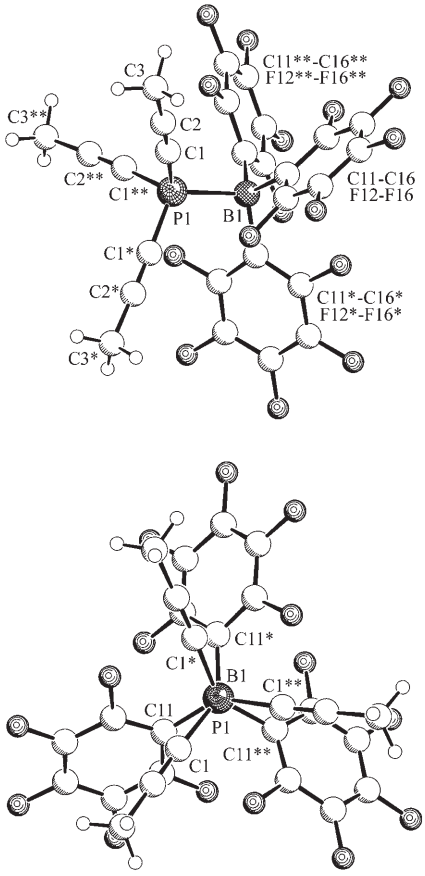

Figure 6. Two views of the molecular structure of **8a**.

conformations depending on the substituents, we performed a series of quantum chemical calculations first on two model compounds PH_3–BH_3 (**9**) and PMe_3–BMe_3 (**10**) and secondly on the real systems **2** and **8(a–c)**, also to elucidate possible crystal-packing effects. For **10** we also computed the potential-energy curve for the P–B bond dissociation. The depth of this potential and the associated force constant are strongly related to the ability for torsion around the B–P bond as, for example, steric interactions between the substituents may be compensated by B–P bond stretching. Before discussing these systems in detail, a closer look at the appropriate quantum chemical methods is necessary.

$H_3B \leftarrow PH_3$ **9** $Me_3B \leftarrow PMe_3$ **10**

The so-called steric interactions between the substituents can be rationalised as the sum of repulsive Pauli and attractive electrostatic and van der Waals (vdW) interactions. The latter are usually not accounted for by standard density functional theory (DFT) methods that are normally used for systems of this size (up to 68 atoms and about 1200 AO basis functions). In our case we have many interatomic distances not far away from those of typical vdW minima (3.5–4.5 Å) and thus, inclusion of vdW effects (the other terms are accounted for quite accurately by DFT) is mandatory. We do this with the recently developed dispersion correction to DFT termed DFT-D,[17a] which has proven very successful in many different chemical applications.[17,18] This approach is used here together with the PBE density functional[19] and its excellent performance for predicting structures and rotational barriers in the P–B system is demonstrated for the two model compounds **9** and **10**. The comparison with reference data obtained at very reliable MP2 and SCS-MP2[20] levels is shown in Table 1.

For the P–B bond lengths, the two methods agree to within 0.01–0.02 Å, while the bond angles are within 0.3°. Note that also the trend when going from the eclipsed to the staggered form (increase of R(P–B) by 0.02–0.03 Å) and the larger effect for R = Me is reproduced accurately by the DFT-D method. Also the rotational barriers agree to within 0.1 kcal mol^{-1}. For **10**, the barrier is about the same as for ethane (2.9 kcal mol^{-1}), but only slightly larger than for **9** (R = H). For **9** the experimental value of the rotational barrier is 2.47 ± 0.05 kcal mol^{-1} .[21] This indicates that (when electronic effects are neglected, for a recent discussion see reference [22]) already the α-carbon atoms are located not far away from regions of attractive vdW interactions. We furthermore determined the torsional barrier for a larger (fixed) B–P distance of 2.22 Å and found a decrease from 2.9 to 1.5 kcal mol^{-1}. This already, at least in part, explains why some compounds may favour the eclipsed conformation: for B–P distances found experimentally (2.05–2.20 Å), the inherent barrier is already so small that attractive vdW interactions between the large substituents can overcompensate.

The potential-energy curves for B–P bond stretching in **10** (all other degrees of freedom fully relaxed at the DFT-D-PBE/TZV(2df,2p) level) are shown in Figure 7. The agreement between DFT-D-PBE and SCS-MP2 is almost perfect,

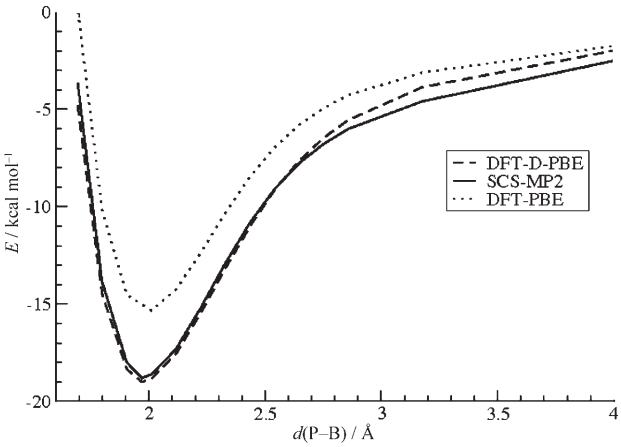

Figure 7. Computed potential-energy curves (TZV(2df,2p) AO basis) for B–P bond stretching of Me_3P–BMe_3 (**10**).

and the importance of the dispersion correction for DFT is also evident from comparison with the plain PBE curve, in which it is seen that it clearly misses some attraction in the minimum region. The dissociation energy is found to be only about 19 kcal mol^{-1}, and around the minimum, bond lengths changes of, for example, 0.3 Å increase the energy by less than 2 kcal mol^{-1}. Thus, this P–B interaction should be considered as quite weak, which explains the wide variations of the P–B distances found experimentally.

The comparison between experimental and computed geometrical parameters that are characteristic for the investigated question are given in Table 2. We do not show all computed geometries here as these are visually not distinguishable from the X-ray data already shown. Perusing this table, one finds that our calculations in all cases predict the right conformer, that is, eclipsed in cases **2** and **8a–c**. The averaged dihedral angles and their trend towards conformer

Table 1. Comparison of structural data [Å, °] and rotational barriers [kcal mol^{-1}] for the two model compounds R_3P–BR_3 **9** (R = H) and **10** (R = Me) at DFT-D-PBE/TZV(2df,2p) and (SCS-)MP2/TZV(2df,2p) levels, respectively.

Method	Conf.	d(B–P)	dihedral angle R-B-P-R	bond angle R-B-P	barrier
10: R = Me					
MP2	**A**	1.962	60.6	105.9	
DFTD-PBE	**A**	1.978	60.5	105.8	
MP2	**B**	2.004	0.0	106.3	2.8[a]
DFTD-PBE	**B**	2.026	0.0	106.2	2.9[b]
9: R = H					
MP2	**A**	1.934	60.2	103.5	
DFTD-PBE	**A**	1.922	60.0	103.7	
MP2	**B**	1.963	0.0	103.7	2.3[a]
DFTD-PBE	**B**	1.947	0.0	104.0	2.3

[a] SCS-MP2 level. [b] The barrier decreases to 1.5 kcal mol^{-1} at a R(P–B) of 2.22 Å.

Table 2. Comparison of calculated (DFT-D-PBE/TZVP′) and experimental structural data for **2** and **8a–c**.[a]

	2		**8c**		**8b**		**8a**	
	exptl	calcd	exptl	calcd	exptl	calcd	exptl	calcd
d(B–P)	2.18	2.22	2.16	2.22	2.13	2.22	2.06	2.18
C-B-P[b]	105	105	114	104	105	103	105	103
C-B-P-C[c]	3.5	0	8.1	1.8	12.3	12.6	20.3	14.7

[a] Bond length in Å, bond angles and dihedral angles in degrees. [b] Average of the three bond angles. [c] Average of the three dihedral angles.

A when phenyl is replaced by the smaller CCMe group is nicely reproduced by our calculations.

For **8a**, we also started the geometry optimisation in conformation **A**, but finally obtained the minimum **B**. This indicates that for these systems only the eclipsed conformation corresponds to a real minimum. We also performed a cross-check and optimised **1** that experimentally prefers conformation **A**, and found also in this case theoretically the right structure. Although crystal packing effects cannot be ruled out, these findings not only support our theoretical treatment, but furthermore indicate that the general phenomenon probably represents an inherent property of the molecules. However, it is also noted that the B–P distances are systematically overestimated by our calculations. Considering the good performance of DFT-D-PBE for the model systems discussed above, this is quite unexpected. Tentatively, these differences between 0.04 and 0.12 Å can be attributed to some "compression" of the structures in the crystal.

But what about the intramolecular vdW interactions mentioned above? These are certainly of importance in the present system but not decisive for the preferred conformation. A first hint comes from computations with the pure PBE functional for which the dispersion correction was switched off. For example, for **8a** we still obtained **B** as a minimum, that is, no qualitative change of the structure was observed. Although the separation of the vdW interaction between the PBE functional and the dispersion correction is only qualitative and one should not take this result too seriously, it points to a different reasoning for the preference of an eclipsed conformation in our systems.

A closer look at the structures in a space-filling model with atomic surfaces drawn at their vdW radius reveals a strong interference of the substituents at phosphorus with the $B(C_6F_6)_3$ group. This is shown for example for **8a** in Figure 8, in which we compare the minimum structure (left) with a hypothetically staggered conformation (dihedral angles adjusted manually to 60° while keeping all other parameters fixed). In Figure 8 (right side), it is seen clearly that this causes clashes of the fluorine atoms with the carbon atoms of the triple bonds. Because the $B(C_6F_6)_3$ group has a strong preference for a propeller-shape due to otherwise too close F···F contacts, the energetically most favoured pathway is thus the torsion around the B–P bond into conformation **B**. A similar explanation holds for the preferred staggered conformation of **1**, where the bulky *tert*-butyl groups on the boron side move in between two phenyl groups on the phosphorous side.

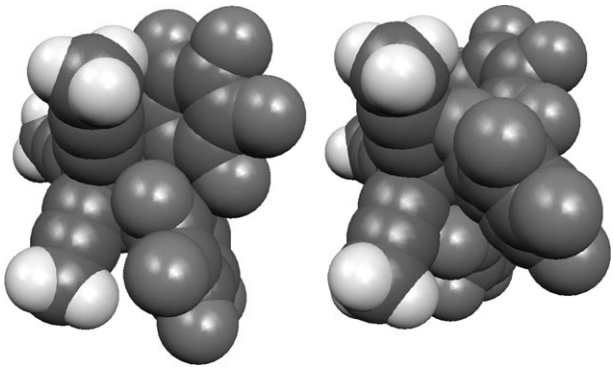

Figure 8. Space-filling model of **8a** in the minimum conformation (left) and a hypothetically staggered form (right).

Conclusion

A systematic series of Lewis acid/Lewis base adducts (**8a–8c**) of $B(C_6F_5)_3$ (**3**) with the propynylphosphines $Ph_2P(C{\equiv}C{-}CH_3)$ (**7c**), $PhP(C{\equiv}C{-}CH_3)_2$ (**7b**), and $P(C{\equiv}C{-}CH_3)_3$ (**7a**) were prepared and their structures in the solid state determined by X-ray diffraction. The adducts **8a–c** all exhibit molecular conformations that are close to eclipsed, with their averaged characteristic dihedral angles θ (C–P–B–C) ranging from 8.1 (**8c**) to 12.3 (**8b**) and 20.3° (**8a**). In a comparison with the preference of typical alkanes for staggered conformations (**A**, $\theta = 60°$) the structural behaviour of the adducts **8** and some similar systems towards favouring the converse eclipsed conformations (**B**, ideal $\theta = 0°$) is striking. From this structural behaviour, which is systematically different from that of the simple alkanes, it is evident that additional attractive and/or repulsive components of interaction between essential subunits of the molecular entities of the adducts **8**, other than the ubiquitous four-electron repulsion between localised bond orbitals, must be held responsible for this unusual behaviour. Our detailed theoretical analysis has revealed the significance of the interplay of additional attractive dispersion forces and specific components of steric hindrance for the qualitative and quantitative description of the specific structural situations encountered in these phosphine–borane addition products. Thus, energetic compensation effects can become quite important for the determination of the favoured structures, especially in systems such as **8**, for which a shallow and soft potential of the P–B bonds favour a rather pronounced response of the overall system to even subtle changes in the periphery. Structural determination by various such secondary effects is probably not limited to such specific systems as the ones used in this combined experimental/theoretical study, but is likely to be encountered more frequently in other systems of a similar topological complexity. It is good to see that recently developed theoretical tools can adequately deal with

the description (and consequently the prediction) of the structural features of such complex molecular systems.[23]

Experimental Section

Materials: All reactions involving air- or moisture-sensitive compounds were carried out under an inert gas atmosphere (Argon) by using Schlenk-type glassware or in a glovebox. Solvents were dried and distilled prior to use. Unless otherwise noted, all starting materials were commercially available and were used without further purification. Propynyllithium[24] and tris(pentafluorophenyl)borane[12] were synthesised according to literature procedure.

Techniques: The following instruments were used for physical characterisation of the compounds: melting points: DSC 2010 TA-instruments; elemental analyses: Foss–Heraeus CHNO-Rapid; NMR: Bruker AC 200 P (^{11}B: 64.2 MHz; ^{31}P: 81 MHz), AMX 300/AV 300 (^{1}H: 300 MHz; ^{13}C: 75 MHz, ^{31}P: 121.5 MHz; ^{19}F: 282.4 MHz), Varian UNITY plus NMR spectrometer (^{1}H: 599.9 MHz; ^{13}C: 150.8 MHz; ^{31}P: 242.8 MHz; ^{19}F: 564.2 MHz).

X-ray crystal structure determinations: Data sets were collected with a Nonius KappaCCD diffractometer equipped with a rotating anode generator. Programs used: data collection COLLECT (Nonius B.V., 1998), data reduction Denzo-SMN,[28], absorption correction SORTAV[29] and Denzo,[30] structure solution SHELXS-97,[31] structure refinement SHELXL-97,[32] graphics SCHAKAL.[33]

CCDC-644001–644006 contain the supplementary crystallographic data for this paper. These data can be obtained free of charge from The Cambridge Crystallographic Data Centre via www.ccdc.cam.ac.uk/data_request/cif.

Allyldi-*tert*-butylphosphine (4a): Allylmagnesium bromide solution in THF (1 M, 33 mL, 33.0 mmol) was added to a mixture of di-*tert*-butylchlorophosphine (5.00 g, 27.6 mmol) in THF (75 mL). The solution was heated for 1 h under reflux. The reaction mixture was concentrated in vacuo until approximately 15 mL remained, then pentane was added (30 mL). After filtration and removal of the solvent in vacuo the residue was distilled under reduced pressure (b.p. 42 °C, 0.25 mbar). A colourless oil was obtained (2.5 g, 49 %). ^{1}H NMR (300 MHz, [D$_2$]dichloromethane, 25 °C, TMS): δ = 5.9 (m, 1H; CH=), 5.01 (m, 2H; =CH$_2$), 2.35 (m, 2H; CH$_2$), 1.2 ppm (d, ^{3}J(P,H) = 13.3 Hz, 12H; *t*Bu); ^{13}C{^{1}H} NMR (76 MHz, [D$_2$]dichloromethane, 25 °C, TMS): δ = 139.6 (d, ^{2}J(P,C) = 16.6 Hz; =CH), 115.2 (d, ^{3}J(P,C) = 10.5 Hz; =CH$_2$), 32.3 (d, ^{1}J(P,C) = 22.5 Hz; *t*Bu), 30.2 (d, ^{2}J(P,C) = 13.5 Hz; *t*Bu), 27.5 ppm (d, ^{1}J(P,C) = 21.4 Hz; CH$_2$); ^{31}P{^{1}H} NMR (122 MHz, [D$_2$]dichloromethane, 25 °C, H$_3$PO$_4$): δ = 60.9 ppm ($\nu_{1/2}$ = 95.2 Hz).

General procedure for the synthesis of alkenyldiphenylphosphines (4b, 4c): Chlorodiphenylphosphine (2 mL, 2.4 g, 10.8 mmol) was dissolved in diethyl ether (100 mL) and cooled down to 0 °C. A solution of the respective enylmagnesium bromide solution (1 equiv) in THF was added at 0 °C. The suspension was stirred for one hour at room temperature. The solid was removed by filtration. The solvent was removed and the product was isolated using vacuum distillation.

Allyldiphenylphosphine (4b): Chlorodiphenylphosphine (2 mL, 10.8 mmol) and 1 M allylmagnesium bromide/THF solution (11 mL, 10.8 mmol) yielded 1.28 g (5.6 mmol, 52 %) of a colourless oil (b.p. 107 °C, oil pump vacuum). ^{1}H NMR (300 MHz, [D$_6$]benzene, 25 °C, TMS): δ = 7.38 (m, 4H; Ph), 7.06 (m, 6H; Ph), 5.77 (m, 1H, =CH), 4.91, 4.89 (2m, 2×H; =CH$_2$), 2.71 ppm (d, ^{3}J(H,H) = 7.4 Hz, 2H; P-CH$_2$); ^{13}C{^{1}H} NMR (76 MHz, [D$_6$]benzene, 25 °C, TMS): δ = 139.0 (d, ^{1}J(P,C) = 16.2 Hz; *i*-Ph), 133.5 (d, ^{2}J(P,C) = 9.6 Hz; CH=), 133.2 (d, ^{2}J(P,C) = 18.6 Hz; *o*-Ph), 128.7 (*p*-Ph), 128.6 (d, ^{3}J(P,C) = 6.5 Hz; *m*-Ph), 117.4 (d, ^{3}J(P,C) = 10.7 Hz; =CH$_2$), 34.0 ppm (d, ^{1}J(P,C) = 14.7 Hz; CH$_2$); ^{31}P{^{1}H} NMR (121 MHz, [D$_6$]benzene, 25 °C, H$_3$PO$_4$): δ = −14.8 ppm ($\nu_{1/2}$=4 Hz).

But-3-enyldiphenylphosphine (4c): Chlorodiphenylphosphine (2 mL, 10.8 mmol) and 0.5 M but-3-enylmagnesium bromide/THF solution (22 mL, 10.8 mmol) yielded 1.53 g (6.4 mmol, 59 %) of a colourless oil (b.p. 130 °C, oil pump vacuum). ^{1}H NMR (300 MHz, [D$_6$]benzene, 25 °C, TMS): δ = 7.39 (m, 4H; Ph), 7.06 (m, 6H; Ph), 5.76 (m, 1H; =CH), 4.92 (m, 2H; =CH$_2$), 2.13, 2.00 ppm (2m, 2×2H; -CH$_2$CH$_2$-); ^{13}C{^{1}H} NMR (76 MHz, [D$_6$]benzene, 25 °C, TMS): δ = 139.5 (d, J(P,C) = 14.6 Hz), 138.9 (d, J(P,C) = 13.6 Hz) (*i*-Ph; CH=), 133.1 (d, ^{2}J(P,C) = 18.8 Hz; *o*-Ph), 128.7 (d, ^{3}J(P,C) ≈ 5.4 Hz; *m*-Ph), 128.6 (*p*-Ph), 114.7 (=CH$_2$), 30.5 (d, ^{1}J(P,C) = 17.1 Hz; PCH$_2$), 27.8 ppm (d, ^{2}J(P,C) = 13.1 Hz; CH$_2$); ^{31}P{^{1}H} NMR (121 MHz, [D$_6$]benzene, 25 °C, H$_3$PO$_4$): δ = −15.0 ppm ($\nu_{1/2}$ = 5 Hz).

General procedure for the synthesis of cyclic phosphine–borane adducts (5a, 5b, 6): Bis(pentafluorophenyl)borane was dissolved in toluene (100 mL) and the enylphosphine (1 equiv) was added. Then the reaction mixture was heated for two hours under reflux. After cooling to room temperature the solvent was removed in oil-pump vacuum. The residue was eluted in pentane (20 mL), isolated by filtration and dried in oil-pump vacuum.

Hydroboration of 4a—formation of 5a: Reaction of bis(pentafluorophenyl)borane (500 mg, 1.45 mmol) and **4a** (271 mg, 1.45 mmol) yielded 217 mg (28 %) of a white solid. ^{1}H NMR (600 MHz, [D$_2$]dichloromethane, 25 °C, TMS): δ = 2.10 (m, 4H; CH$_2$-CH$_2$-P), 1.69 (m, 2H; CH$_2$-B), 1.25 ppm (d, ^{3}J(P,H) = 12.5 Hz, 18H; *t*Bu); ^{13}C{^{1}H} NMR (151 MHz, [D$_2$]dichloromethane, 25 °C, TMS): δ = 148.1 (dm, ^{1}J(F,C) = 244 Hz; *o*-C$_6$F$_5$), 139.7 (dm, ^{1}J(F,C) = 240 Hz; *p*-C$_6$F$_5$), 137.6 (dm, ^{1}J(F,C) = 248 Hz; *m*-C$_6$F$_5$), 122.9 (m; *i*-C$_6$F$_5$), 35.4 (d, ^{1}J(P,C) = 15.8 Hz; *t*Bu), 29.9 (s; *t*Bu), 22.3 (br; BCH$_2$), 21.8 (d, ^{1}J(P,C) = 37.5 Hz; PCH$_2$), 21.1 ppm (d, ^{2}J(P,C) = 10.9 Hz; CH$_2$); ^{19}F NMR (564 MHz, [D$_2$]dichloromethane, 25 °C, CFCl$_3$): δ = −128.5 (br; *o*-C$_6$F$_5$), −159.5 (*p*-C$_6$F$_5$), −165.0 ppm (*m*-C$_6$F$_5$); ^{31}P{^{1}H} NMR (122 MHz, [D$_2$]dichloromethane, 25 °C, H$_3$PO$_4$): δ = 42 ppm ($\nu_{1/2}$ = 140 Hz); ^{11}B{^{1}H} NMR (160 MHz, [D$_2$]dichloromethane, 25 °C, BF$_3$OEt$_2$): δ = −10 ppm (d, ^{1}J(P,B) ≈ 50 Hz, $\nu_{1/2}$ = 70 Hz); elemental analysis calcd (%) for C$_{23}$H$_{24}$BF$_{10}$P: C 51.91, H 4.55; found: C 51.82, H 4.25.

X-ray crystal structure analysis of ***5a***: formula C$_{23}$H$_{24}$BF$_{10}$P, M_r = 532.20, colourless crystal 0.40×0.30×0.10 mm, a = 9.5439(2), b = 10.2216(2), c = 13.4103(3) Å, α = 70.592(1). β = 71.347(2), γ = 72.095(1)°, V = 1139.07(4) Å^3, ρ_{calcd} = 1.552 g cm^{-3}, μ = 0.213 mm^{-1}, empirical absorption correction (min/max transmission: 0.920/0.979), Z = 2, triclinic, space group $P\bar{1}$ (No. 2), λ = 0.71073 Å, T = 198 K, ω and ϕ scans, 12463 reflections collected ($\pm h$, $\pm k$, $\pm l$), [(sinθ)/λ] = 0.67 Å^{-1}, 5470 independent (R_{int} = 0.037) and 4691 observed reflections [$I \geq 2\sigma(I)$], 322 refined parameters, R = 0.037, wR^2 = 0.104, max/min residual electron density 0.34/−0.34 e Å^{-3}, hydrogen atoms calculated and refined as riding atoms.

Hydroboration of 4b—formation of 5b: Bis(pentafluorophenyl)borane (1.25 g, 3.6 mmol) and **4b** (0.82 g, 3.6 mmol) yielded 1.05 g (1.8 mmol, 51 %) of a white solid, m.p. 140 °C (DSC). ^{1}H NMR (600 MHz, [D$_6$]benzene, 25 °C, TMS): δ = 6.98 (m, 4H, *o*-Ph), 6.90 (m, 2H, *p*-Ph), 6.79 (m, 4H, *m*-Ph), 2.05 (m, 4H, CH$_2$-CH$_2$-P), 1.86 ppm (m, 2H; CH$_2$-B); ^{13}C{^{1}H} NMR (151 MHz, [D$_6$]benzene, 25 °C, TMS): δ = 148.3 (dm, ^{1}J(F,C) = 240 Hz; *o*-C$_6$F$_5$), 139.7 (dm, ^{1}J(F,C) = 250 Hz; *p*-C$_6$F$_5$), 137.4 (dm, ^{1}J(F,C) = 248 Hz; *m*-C$_6$F$_5$), 132.0 (d, ^{2}J(P,C) = 8.1 Hz; *o*-Ph), 131.4 (d, ^{4}J(P,C) = 2.8 Hz; *p*-Ph), 128.7 (d, ^{3}J(P,C) = 10.2 Hz; *m*-Ph), 127.8 (d, ^{1}J(P,C) = 50.3 Hz; *i*-Ph), 119.6 (br; *i*-C$_6$F$_5$), 27.2 (d, ^{1}J(P,C) = 42.6 Hz; PCH$_2$), 25.6 (d, ^{2}J(P,C) = 14.8 Hz; CH$_2$), 23.7 ppm (br; CH$_2$-B); ^{19}F NMR (564 MHz, [D$_6$]benzene, 25 °C, CFCl$_3$): δ = −129.5 (*o*-C$_6$F$_5$), −158.5 (*p*-C$_6$F$_5$), −164.2 ppm (*m*-C$_6$F$_5$); ^{31}P{^{1}H} NMR (243 MHz, [D$_6$]benzene, 25 °C, H$_3$PO$_4$): δ = 22.6 ppm ($\nu_{1/2}$ = 80 Hz); ^{11}B{^{1}H} NMR (96 MHz, [D$_6$]benzene, 25 °C, BF$_3$OEt$_2$): δ = −9 ppm ($\nu_{1/2}$ = 180 Hz); elemental analysis calcd (%) for C$_{27}$H$_{16}$BF$_{10}$P: C 56.68, H 2.82; found: C 56.86, H 2.99.

X-ray crystal structure analysis of ***5b***: formula C$_{27}$H$_{16}$BF$_{10}$P, M_r = 572.18, colourless crystal 0.40×0.25×0.15 mm, a = 8.928(1), b = 11.558(1), c = 13.358(1) Å, α = 66.15(1). β = 84.05(1), γ = 68.74(1)°, V = 1173.4(2) Å^3, ρ_{calcd} = 1.619 g cm^{-3}, μ = 0.213 mm^{-1}, empirical absorption correction (min/max transmission: 0.920/0.969), Z = 2, triclinic, space group $P\bar{1}$ (No. 2), λ = 0.71073 Å, T = 198 K, ω and ϕ scans, 10859 reflections collected ($\pm h$, $\pm k$, $\pm l$), [(sinθ)/λ] = 0.67 Å^{-1}, 5590 independent (R_{int} = 0.032) and 4227 observed reflections [$I \geq 2\sigma(I)$], 352 refined parameters, R = 0.042,

$wR^2 = 0.105$, max/min residual electron density 0.38/−0.36 e Å^{-3}, hydrogen atoms calculated and refined as riding atoms.

Hydroboration of 4c—formation of 6: Bis(pentafluorophenyl)borane (1.44 g, 4.1 mmol) and **4c** (1.00 g, 4.1 mmol) yielded 1.58 g (2.7 mmol, 66%) of a white solid, m.p. 143°C (DSC). ^{1}H NMR (600 MHz, [D$_2$]dichloromethane, 25°C, TMS): $\delta = 7.49$, 7.38 (2m, 10H; Ph), 2.64 (dt, ^3J(H,H) = 6.7 Hz, ^2J(P,H) = 11.5 Hz, 2H; PCH_2), 1.98 (br, 2H; CH_2), 1.57 ppm (br, 4H; -CH_2-CH_2B); ^{13}C{^{1}H} NMR(101 MHz, [D$_2$]dichloromethane, 25°C, TMS): $\delta = 148.2$ (dm, ^1J(F,C) = 239 Hz; *o*-C_6F_5), 139.5 (dm, ^1J(F,C) = 234 Hz; *p*-C_6F_5), 137.4 (dm, ^1J(F,C) = 256 Hz; *m*-C_6F_5), 133.0 (d, ^3J(P,C) = 8.2 Hz; *o*-Ph), 131.7 (d, ^4J(P,C) = 2.5 Hz; *p*-Ph), 130.0 (d, ^1J(P,C) = 54.0 Hz; *i*-Ph), 129.0 (d, ^2J(P,C) = 10.0 Hz; *m*-Ph), 120.4 (br; *i*-C_6F_5), 25.5 (d, ^2J(P,C) = 3.6 Hz; $^{PCH_2}CH_2$), 24.6 (d, ^3J(P,C) = 7.7 Hz; $CH_2^{CH_2B}$), 23.5 (d, ^1J(P,C) = 32.2 Hz; PCH_2), 19.6 ppm (br; BCH_2); ^{19}F NMR (564 MHz, [D$_2$]dichloromethane, 25°C, $CFCl_3$): $\delta = -128.4$ (br; *o*-C_6F_5), −157.8 (*p*-C_6F_5), −163.0 ppm (*m*-C_6F_5); ^{31}P{^{1}H} NMR(121 MHz, [D$_2$]dichloromethane, 25°C, H_3PO_4): $\delta = 0.5$ ppm ($\nu_{1/2} = 120$ Hz); ^{11}B{^{1}H} NMR (64 MHz, [D$_2$]dichloromethane, 25°C, BF_3OEt_2): $\delta = -12$ ppm ($\nu_{1/2}$=164 Hz); elemental analysis calcd (%) for $C_{28}H_{18}BF_{10}P$: C 57.37, H 3.09; found: C 57.60, H 3.32. For the determination of the Gibbs activation energies equation $\Delta G^{\neq}(T_C,\Delta\nu(T)) = RT_C(22.96+\ln(T_c/\Delta\nu)$ was used with the following parameters : ring inversion process: $\Delta G^{\neq}_{inv}$ (243 K, 511 Hz (188 K)) = 10.7 ± 0.5 kcal mol^{-1}; rotation barrier of the first B-C_6F_5 unit: $\Delta G^{\neq}_{rot}$ (275 K, 4320 Hz (188 K)) = 11.0 ± 0.5 kcal mol^{-1}).

X-ray crystal structure analysis of ***6***: formula $C_{28}H_{18}BF_{10}P$, $M_r = 586.20$, colourless crystal 0.15 × 0.10 × 0.03 mm, $a = 9.451(1)$, $b = 10.780(1)$, $c = 13.504(1)$ Å, $\alpha = 83.21(1)$. $\beta = 76.56(1)$, $\gamma = 68.09(1)°$, $V = 1240.7(2)$ Å^3, $\rho_{calcd} = 1.569$ g cm^{-3}, $\mu = 0.204$ mm^{-1}, empirical absorption correction (min/max transmission: 0.970/0.994), $Z = 2$, triclinic, space group $P\bar{1}$ (No. 2), $\lambda = 0.71073$ Å, $T = 223$ K, ω and ϕ scans, 11 642 reflections collected ($\pm h$, $\pm k$, $\pm l$), [(sinθ)/λ] = 0.67 Å^{-1}, 5897 independent ($R_{int} = 0.046$) and 3723 observed reflections [$I \geq 2\sigma(I)$], 361 refined parameters, $R = 0.057$, $wR^2 = 0.124$, max/min residual electron density 0.28/−0.38 e Å^{-3}, hydrogen atoms calculated and refined as riding atoms.

General procedure for the synthesis of alkynylphosphines (7a–c):[7–11] A suspension of propynyl lithium (1 equiv) in THF (100 mL) was cooled to −78°C. The molar equivalent of the respective chlorophosphine was added and the resulting brown solution was stirred for one hour without a cooling bath. For workup, the solvent was evaporated and the product was extracted (under argon) with dry diethyl ether (3 × 30 mL) by using a filter canula. The ether layer was evaporated to dryness and the product was isolated by distillation or sublimation.

Diphenylpropynylphosphine (7c):[9] Reaction of propynyl lithium (1.20 g, 26.1 mmol) with chlorodiphenylphosphine (4.5 mL, 24.4 mmol) yielded **7c** (2.85 g, 52%) as a colourless oil, which becomes a solid after a few hours. The product was purified by distillation (b.p. 150°C, oil pump vacuum). ^{1}H NMR (400 MHz, [D$_6$]benzene, 25°C, TMS): $\delta = 7.72$ (m, 4H; Ph), 7.07, 7.02 (2m, 6H; Ph), 1.53 ppm (d, ^4J(P,H) = 1.5 Hz, 3H; CH_3); ^{13}C{^{1}H} NMR (101 MHz, [D$_6$]benzene, 25°C, TMS): $\delta = 137.7$ (d, ^1J(P,C) = 7.6 Hz; *i*-Ph), 132.9 (d, ^2J(P,C) = 21.0 Hz; *o*-Ph), 129.0 (*p*-Ph), 128.8 (d, ^3J(P,C) = 7.7 Hz; *m*-Ph), 106.0 (d, ^2J(P,C) = 4.5 Hz; ≡*C*CH$_3$), 76.1 (d, ^1J(P,C) = 3.3 Hz; P*C*≡), 4.9 ppm (d, ^3J(P,C) = 1.1 Hz, CH_3); ^{31}P{^{1}H} NMR (121.5 MHz, [D$_6$]benzene, 25°C, TMS): $\delta = -32.0$ ppm ($\nu_{1/2}$=3 Hz); IR (KBr): $\tilde{\nu} = 2183$ cm^{-1} (vs, C≡C).

Phenyldipropynylphosphine (7b):[10] Reaction of propynyl lithium (1.17 g, 25.4 mmol) with dichlorophenylphosphine (1.35 mL, 10.3 mmol) yielded **7b** (2.85 g, 66%) as a colourless oil. The product was purified by distillation (b.p. 135°C, oil pump vacuum). ^{1}H NMR (300 MHz, [D$_6$]benzene, 25°C, TMS): $\delta = 7.98$ (m, 2H; Ph), 7.23, 7.15 (2m, 3H; Ph), 1.56 ppm (d, ^4J(P,H) = 1.9 Hz, 6H; CH_3); ^{13}C{^{1}H} NMR (75 MHz, [D$_6$]benzene, 25°C, TMS): $\delta = 135.3$ (*i*-Ph), 132.4 (d, ^{2}J(P,C) = 22.3 Hz; *o*-Ph), 129.3 (*p*-Ph), 128.8 (d, ^{3}J(P,C) = 7.9 Hz; *m*-Ph) 104.2 (d, ^{2}J(P,C) = 6.6 Hz; ≡*C*CH$_3$), 74.1 (P*C*≡), 4.8 ppm (CH_3); ^{31}P{^{1}H} NMR (121 MHz, [D$_6$]benzene, 25°C, H_3PO_4): $\delta = -43.0$ ppm ($\nu_{1/2}$ = 20 Hz). IR (KBr): $\tilde{\nu} = 2182$ cm^{-1} (vs, C≡C).

Tripropynylphosphine (7a):[11,9c] Reaction of propynyl lithium (2.12 g, 46.1 mmol) with phosphorustrichloride (1.3 mL, 15.4 mmol) yielded **7a** (1.32 g, 58%) as a white solid. The product was purified by sublimation (100°C, oil pump vacuum). ^{1}H NMR (300 MHz, [D$_6$]benzene, 25°C, TMS): $\delta = 1.40$ ppm (d, ^4J(P,H) = 2.3 Hz, 9H; CH_3); ^{13}C{^{1}H} NMR (101 MHz, [D$_6$]benzene, 25°C, TMS): $\delta = 103.3$ (d, ^2J(P,C) = 10.8 Hz; ≡CCH_3), 71.5 (d, ^1J(P,C) = 9.4 Hz; P*C*≡), 4.6 ppm (CH_3); ^{31}P{^{1}H} NMR (121.5 MHz, [D$_6$]benzene, 25°C, H_3PO_4): $\delta = -86.3$ ppm ($\nu_{1/2}$ = 10 Hz); IR (KBr): $\tilde{\nu} = 2189$ cm^{-1} (vs, C≡C).

Diphenylpropynylphosphine–tris(pentafluorophenyl)borane adduct (8c): Tris(pentafluorophenyl)borane (0.67 g, 1.3 mmol) and diphenylpropynylphosphine (0.29 g, 1.3 mmol) were dissolved in toluene (30 mL). The reaction mixture was stirred for 2 h at ambient temperature. The solvent was removed until 5 mL remained in the flask. Pentane (20 mL) was added and the product started to precipitate as a white solid. It was collected by filtration, washed with pentane (3 mL) and dried in vacuum to yield **8c** (0.75 g, 78%). M.p. 140°C (DSC, decomp); ^{1}H NMR (600 MHz, [D$_2$]dichloromethane, 25°C, TMS): $\delta = 7.50$ (m, 6H; Ph), 7.35 (m, 4H; Ph), 2.00 ppm (d, ^4J(P,H) = 4.0 Hz, 3H; CH_3); ^{13}C{^{1}H} NMR (151 MHz, [D$_2$]dichloromethane, 25°C, TMS): $\delta = 148.8$ (dm, ^1J(F,C) = 242 Hz; *o*-C_6F_5), 140.6 (dm, ^1J(F,C) = 251 Hz; *p*-C_6F_5), 137.3 (dm, ^1J(F,C) = 255 Hz; *m*-C_6F_5), 133.2 (d, ^3J(P,C) = 9.6 Hz; *o*-Ph), 132.3 (d, ^4J(P,C) = 2.8 Hz; *p*-Ph), 129.0 (d, ^2J(P,C) = 11.1 Hz; *m*-Ph), 126.2 (d, ^1J(P,C) = 58.0 Hz; *i*-Ph), 115.6 (br; *i*-C_6F_5), 113.2 (d, ^2J(P,C) = 15.4 Hz; ≡C−), 67.1 (d, ^1J(P,C) = 119.3 Hz; P*C*≡), 5.4 ppm (d, ^4J(P,C) = 2.9 Hz; CH_3); ^{31}P{^{1}H} NMR (121 MHz, [D$_2$]dichloromethane, 25°C, H_3PO_4): δ = 6.4 ppm ($\nu_{1/2}$ = 85 Hz); ^{11}B{^{1}H} NMR (64 MHz, [D$_2$]dichloromethane, 25°C, BF_3OEt_2): $\delta = -8$ ppm ($\nu_{1/2}$ = 220 Hz); ^{19}F NMR (282 MHz, [D$_2$]dichloromethane, 25°C, $CFCl_3$): $\delta = -125.1$ (*o*-C_6F_5), −155.1 (*p*-C_6F_5), −163.1 ppm (*m*-C_6F_5); IR (KBr): $\tilde{\nu} = 2211$ cm^{-1} (vs, C≡C); elemental analysis calcd (%) for $C_{33}H_{13}BF_{15}P$: C 53.84, H 1.78; found: C 53.48, H 1.95.

X-ray crystal structure analysis of ***8c***: Single crystals were obtained from diethyl ether, formula $C_{33}H_{13}BF_{15}P$, $M_r = 736.21$, yellow crystal 0.20 × 0.15 × 0.15 mm, $a = 10.251(1)$, $b = 11.515(1)$, $c = 13.523(1)$ Å, $\alpha = 85.89(1)$, $\beta = 75.16(1)$, $\gamma = 73.11(1)°$, $V = 1476.5(2)$ Å^3, $\rho_{calcd} = 1.656$ g cm^{-3}, $\mu = 0.214$ mm^{-1}, empirical absorption correction (min/max transmission: 0.959/0.969), $Z = 2$, triclinic, space group $P\bar{1}$ (No. 2), $\lambda = 0.71073$ Å, $T = 198$ K, ω and ϕ scans, 18 013 reflections collected ($\pm h$, $\pm k$, $\pm l$), [(sinθ)/λ] = 0.62 Å^{-1}, 5981 independent ($R_{int} = 0.052$) and 3327 observed reflections [$I \geq 2\sigma(I)$], 452 refined parameters, $R = 0.056$, $wR^2 = 0.137$, max/min residual electron density 0.61/−0.34 e Å^{-3}, hydrogen atoms calculated and refined as riding atoms.

Phenyldipropynylphosphine–tris(pentafluorophenyl)borane adduct (8b): Tris(pentafluorophenyl)borane (0.67 g, 1.30 mmol) was dissolved in toluene (30 mL). Phenyldipropynylphosphine (0.24 g, 1.30 mmol) was added and the reaction mixture stirred for 2 h at ambient temperature. The solvent was removed until 5 mL remained in the flask. Pentane (20 mL) was added and the product started to precipitate as a white solid. It was collected by filtration, washed with pentane (3 mL) and dried in vacuum to yield **8b** (0.30 g, 54%) as a white solid. M.p. 147°C (DSC, decomp); ^{1}H NMR (600 MHz, [D$_2$]dichloromethane, 25°C, TMS): $\delta = 7.75$ (m, 2H; *o*-Ph), 7.51 (m, 1H; *p*-Ph), 7.41 (m, 2H; *o*-Ph), 1.98 ppm (d, ^4J(P,H) = 4.1 Hz, 6H; CH_3); ^{13}C{^{1}H} NMR (151 MHz, 600 MHz, [D$_2$]dichloromethane, 25°C, TMS): $\delta = 149.1$ (dm, ^1J(F,C) = 240 Hz; *o*-C_6F_5), 140.6 (dm, ^1J(F,C) = 251 Hz; *p*-C_6F_5), 137.3 (dm, ^1J(F,C) = 249 Hz; *m*-C_6F_5), 132.7 (d, ^2J(P,C) ≈ 10 Hz; *o*-Ph), 132.69 (br; *p*-Ph), 129.0 (d, ^3J-(P,C) = 12.1 Hz; *m*-Ph), 124.1 (d, ^1J(P,C) = 70.9 Hz; *i*-Ph), 115.3 (br; *i*-C_6F_5), 110.5 (d, ^2J(P,C) = 20.1 Hz; ≡C−), 65.5 (d, ^1J(P,C) = 134.9 Hz; P*C*≡), 5.3 ppm (d, ^4J(P,C) = 3.0 Hz; Me); ^{31}P{^{1}H} NMR (243 MHz, [D$_2$]dichloromethane, 25°C, H_3PO_4): $\delta = -15$ ppm ($\nu_{1/2}$ = 130 Hz); ^{11}B{^{1}H} NMR (64 MHz, [D$_2$]dichloromethane, 25°C, BF_3OEt_2): δ = −7 ppm ($\nu_{1/2}$ = 310 Hz); ^{19}F NMR (564 MHz, [D$_2$]dichloromethane, 25°C, $CFCl_3$): $\delta = -127.3$ (*o*-C_6F_5), −157.2 (br, *p*-C_6F_5), −165.3 ppm (*m*-C_6F_5); IR(KBr): $\tilde{\nu} = 2204$ cm^{-1} (vs, C≡C); elemental analysis calcd (%) for $C_{30}H_{11}BF_{15}P$: C 51.61, H 1.59; found: C 51.23, H 1.62.

X-ray crystal structure analysis of ***8b***: Single crystals were obtained from diethyl ether, formula $C_{30}H_{11}BF_{15}P$, $M_r = 698.17$, colourless crystal 0.30 × 0.30 × 0.15 mm, $a = 10.707(1)$, $b = 11.438(1)$, $c = 11.566(1)$ Å, $\alpha = 91.71(1)$, $\beta = 101.31(1)$, $\gamma = 93.91(1)°$, $V = 1384.4(2)$ Å^3, $\rho_{calcd} = 1.675$ g cm^{-3}, μ =

0.223 mm^{-1}, empirical absorption correction (min/max transmission 0.936/0.967), $Z=2$, triclinic, space group $P\bar{1}$ (No. 2), $\lambda=0.71073$ Å, $T=198$ K, ω and ϕ scans, 15421 reflections collected ($\pm h$, $\pm k$, $\pm l$), [$(\sin\theta)/\lambda$] = 0.67 Å^{-1}, 6709 independent ($R_{int}=0.039$) and 5084 observed reflections [$I \geq 2\sigma(I)$], 426 refined parameters, $R=0.045$, $wR^2=0.119$, max/min residual electron density 0.34/−0.31 e Å^{-3}, hydrogen atoms calculated and refined as riding atoms.

Tripropynylphosphine–tris(pentafluorophenyl)borane-adduct (8a): Tris(pentafluorophenyl)borane (0.67 g, 1.30 mmol) and tripropynylphosphine (0.19 g, 1.30 mmol) were dissolved in toluene (30 mL). The reaction mixture was stirred for 2 h at ambient temperature. The solvent was removed until 5 mL remained in the flask. Pentane (20 mL) was added and the product started to precipitate as a white solid. It was collected by filtration, washed with pentane (3 mL) and dried in vacuum to yield **8a** (0.54 g, 63%) as a white solid. M.p. 160°C (DSC, decomp); ^{1}H NMR (600 MHz, [D$_2$]dichloromethane, 25°C, TMS): $\delta=1.92$ ppm (d, ^4J(P,H) = 4.2 Hz; CH_3); ^{13}C{^{1}H} NMR (151 MHz, [D$_2$]dichloromethane, 25°C, TMS): $\delta=149.2$ (dm, ^1J(F,C) = 240 Hz; *o*-C_6F_5), 140.6 (dm, ^1J(F,C) = 248 Hz; *p*-C_6F_5), 137.4 (dm, ^1J(F,C) = 250 Hz; *m*-C_6F_5), 115.0 (br, *i*-C_6F_5), 108.9 (d, ^2J(P,C) = 25.6 Hz; ≡C−), 64.1 (d, ^1J(P,C) = 156.8 Hz; PC≡), 5.2 ppm (d, ^3J(P,C) = 3.5 Hz; CH_3); ^{31}P{^{1}H} NMR (121 MHz, [D$_2$]dichloromethane, 25°C, H_3PO_4): $\delta=-38.0$ ppm ($\nu_{1/2}=150$ Hz); ^{11}B{^{1}H} NMR (64 MHz, [D$_2$]dichloromethane, 25°C, BF_3OEt_2): $\delta=-9$ ppm ($\nu_{1/2}=200$ Hz); ^{19}F NMR (282 MHz, [D$_2$]dichloromethane, 25°C, $CFCl_3$): $\delta=-126.0$ (*o*-C_6F_5), −155.2 (*p*-C_6F_5), −163.2 ppm (*m*-C_6F_5); IR-(KBr): $\tilde{\nu}=2217$ cm^{-1} (vs, C≡C); elemental analysis calcd (%) for $C_{27}H_9BF_{15}P$: C 49.13, H 1.37; found: C 48.95, H 1.68.

X-ray crystal structure analysis of ***8a***: Single crystals were obtained from diethyl ether, formula $C_{27}H_9BF_{15}P$, $M_r=660.12$, colourless crystal 0.30 × 0.25 × 0.20 mm, $a=17.629(1)$, $b=17.629(1)$, $c=15.180(1)$ Å, $\alpha=90.00$, $\beta=90.00$, $\gamma=120.00°$, $V=4085.6(4)$ Å^3, $\rho_{calcd}=1.610$ g cm^{-3}, $\mu=0.221$ mm^{-1}, empirical absorption correction (min/max transmission0.937/0.957), $Z=6$, hexagonal, space group $R\bar{3}$ (No. 148), $\lambda=0.71073$ Å, $T=198$ K, ω and ϕ scans, 4893 reflections collected ($\pm h$, $\pm k$, $\pm l$), [$(\sin\theta)/\lambda$] = 0.66 Å^{-1}, 2140 independent ($R_{int}=0.027$) and 1542 observed reflections [$I \geq 2\sigma(I)$], 134 refined parameters, $R=0.041$, $wR^2=0.114$, max/min residual electron density 0.17/−0.25 e Å^{-3}, hydrogen atoms calculated and refined as riding atoms.

Theoretical methods used: The quantum chemical calculations were performed with slightly modified versions of the TURBOMOLE suite of programs.[25] As AO basis, triple-zeta (TZV) sets of Ahlrichs et al.[26] were employed. In the calculations of the model compounds, (2df,2p) polarisation functions were added. For the real systems (2df) polarisation functions were used only for the phosphorus and boron atoms, while for all other atoms a smaller (d,p) set was used. This basis was denoted as TZVP′. In the (SCS-)MP2 treatments for the correlation energy (frozen-core approximation) and for the Coulomb operator in the DFT treatments, the RI-approximation and the m4 numerical quadrature grid were used.[27] For a detailed description of the dispersion correction used together with the PBE[19] density functional (termed DFT-D-PBE), see reference [17a]). The geometries of **2** and **5a–c** were fully optimised at the corresponding theoretical level without any symmetry restrictions. In the model calculations and for the potential energy curves, the C_{3v} or C_3 symmetry, respectively, was used. As starting geometries, in most cases the experimental X-ray structures were employed, which ensured that the right minima with respect to rotations of the substituents were computed. In selected cases, cross-checks were made by optimisations started from conformers with rotations around the B−P bond.

Acknowledgements

Financial support from the Deutsche Forschungsgemeinschaft and the Fonds der Chemischen Industrie is gratefully acknowledged. We thank the BASF AG for the generous donation of solvents.

[1] E. L. Eliel, S. H. Wilen, M. P. Doyle, *Basic Organic Stereochemistry*, Wiley, New York, **2001**.
[2] a) V. Pophristic, L. Goodman, *Nature* **2001**, *411*, 565–568; b) F. M. Bickelhaupt, E. J. Baerends, *Angew. Chem.* **2003**, *115*, 4315–4320; *Angew. Chem. Int. Ed.* **2003**, *42*, 4183–4188; c) F. Weinhold, *Angew. Chem.* **2003**, *115*, 4320–4326; *Angew. Chem. Int. Ed.* **2003**, *42*, 4188–4194.
[3] a) C. F. Matta, J. Hernández-Trujillo, T. H. Tang, R. F. W. Bader, *Chem. Eur. J.* **2003**, *9*, 1940–1951; b) J. Poater, M. Solà, F. M. Bickelhaupt, *Chem. Eur. J.* **2006**, *12*, 2889–2895; c) R. F. W. Bader, *Chem. Eur. J.* **2006**, *12*, 2896–2901; d) J. Poater, M. Solà, F. M. Bickelhaupt, *Chem. Eur. J.* **2006**, *12*, 2902–2905.
[4] M. J. Bayer, H. Pritzkow, W. Siebert, *Eur. J. Inorg. Chem.* **2002**, 2069–2072.
[5] H. Jacobsen, H. Berke, S. Döring, G. Kehr, G. Erker, R. Fröhlich, O. Meyer, *Organometallics* **1999**, *18*, 1724–1735.
[6] a) S. Hietkamp, D. J. Stufkens, K. Vrieze, *J. Organomet. Chem.* **1976**, *112*, 419–428; b) W. E. Piers, T. Chivers, *Chem. Soc. Rev.* **1997**, *26*, 345–354.
[7] a) J. H. Williams, *Acc. Chem. Res.* **1993**, *26*, 593–598; b) S. L. Cockroft, C. A. Hunter, K. R. Lawson, J. Perkins, C. J. Urch, *J. Am. Chem. Soc.* **2005**, *127*, 8594–8595; c) Y. El-azizi, A. Schmitzer, S. K. Collins, *Angew. Chem.* **2006**, *118*, 982–987; *Angew. Chem. Int. Ed.* **2006**, *45*, 968–973; and references cited in these articles.
[8] a) W. Ahlers, B. Temme, G. Erker, R. Fröhlich, T. Fox, *J. Organomet. Chem.* **1997**, *527*, 191–201; b) D. Vagedes, G. Erker, G. Kehr, K. Bergander, O. Kataeva, R. Fröhlich, S. Grimme, C. Mück-Lichtenfeld, *Dalton Trans.* **2003**, 1337–1344; c) S. Guidotti, I. Camurati, F. Focante, L. Angellini, G. Moscardi, L. Resconi, R. Leardini, D. Nanni, P. Mercandelli, A. Sironi, T. Beringhelli, D. Maggioni, *J. Org. Chem.* **2003**, *68*, 5445–5465; d) F. Focante, R. Leardini, A. Mazzanti, P. Mercandelli, D. Nanni, *Organometallics* **2006**, *25*, 2166–2172.
[9] a) C. Charrier, W. Chodkiewicz, P. Cadiot, *Bull. Soc. Chim. France* **1966**, *167*, 1002–1011; b) M. Simalty, M. H. Mebazaa, *Bull. Soc. Chim. France* **1972**, *554*, 3532–3536; c) R.-M. Lequan, M.-J. Pouet, M.-P Simonnin, *Org. Magn. Reson.* **1975**, 392–400; d) C. Charrier, M.-P Simonnin, W. Chodkiewicz, P. Cadiot, *Compt. Rend. Acad. Sci. Paris* **1964**, *258*, 1537–2540.
[10] a) W. E. Davidsohn, M. C. Henry, *Chem. Rev.* **1967**, *67*, 73–106; b) G. Märkl, W. Weber, W. Weiss, *Chem. Ber.* **1985**, *118*, 2365–2395.
[11] a) W. R. Cullen, D. C. Frost, W. R. Leeder, *J. Fluorine Chem.* **1971**, *1*, 227–233; b) R. E. Sacher, B. C. Pant, F. A. Miller, F. R. Brown, *Spectrochim. Acta, Part A* **1972**, *28*, 1361–1373.
[12] a) A. G. Massey, A. J. Park, F. G. A. Stone, *Proc. Chem. Soc.* **1963**, *212*; b) A. G. Massey, A. J. Park, *J. Organomet. Chem.* **1964**, *2*, 245–250; c) J. L. Pohlmann, F. E. Brinkmann, *Z. Naturforsch. B* **1965**, *20*, 1–4; d) J. L. Pohlmann, F. E. Brinkmann, *Z. Naturforsch. B* **1965**, *20*, 5–11; e) A. G. Massey, A. J. Park, *J. Organomet. Chem.* **1966**, *5*, 218–225.
[13] For other examples of B(C_6F_5)$_3$-phosphine adducts and related compounds see e.g.: a) D. C. Bradely, M. B. Hursthouse, M. Motevalli, Z. Dao-Hong, *J. Chem. Soc. Chem. Commun.* **1991**, 7–8; b) D. C. Bradely, I. S. Harding, A. D. Keefe, M. Motevalli, D. H. Zheng, *J. Chem. Soc. Dalton Trans.* **1996**, 3931–3936; c) B. E. Carpenter, W. E. Piers, R. McDonald, *Can. J. Chem.* **2001**, *79*, 291–295; d) B. E. Carpenter, W. E. Piers, M. Parvez, G. P. A. Yap, S. J. Rettig, *Can. J. Chem.* **2001**, *79*, 857–867; e) J. M. Denis, H. Forintos, H. Szelke, L. Toupet, T.-N. Pham, P.-J. Madec, A.-C. Gaument, *Chem. Commun.* **2003**, 54–55; see also reference [5], and references therein.
[14] Structures of other related examples of R_3P–BR_3 adducts: a) M. S. Lube, R. L. Wells, *Inorg. Chem.* **1996**, *35*, 5007–5014; b) R. B. Coapes, F. E. S. Souza, M. A. Fox, A. S. Batsanov, A. E. Goeta, D. S. Yufit, M. A. Leech, J. A. K. Howard, A. J. Scott, W. Clegg, T. B. Marder, *J. Chem. Soc. Dalton Trans.* **2001**, 1201–1209; c) T. J. Malefetse, G. J. Swiegers, N. J. Coville, M. A. Fernandes, *Organometallics* **2002**, *21*, 2898–2904; d) N. Oohara, T. Imamoto, *Bull. Chem. Soc. Jpn.* **2002**, *75*, 1359–1365; e) U. Monkowius, S. Nogai, H. Schmidbaur, *Dalton Trans.* **2003**, 987–991.

[15] For the structures of other representative examples of Lewis base-B-$(C_6F_5)_3$ adducts see e.g.: a) D. Röttger, G. Erker, R. Fröhlich, S. Kotila, *J. Organomet. Chem.* **1996**, *518*, 17–19; b) J. R. Galsworthy, M. L. H. Green, M. Müller, K. Prout, *J. Chem. Soc. Dalton Trans* **1997**, 1309–1313; c) M. J. G. Lesly, A. Woodward, N. J. Taylor, T. B. Marder, *Chem. Mater.* **1998**, *10*, 1355–1365; d) S. Döring, G. Erker, R. Fröhlich, O. Meyer, K. Bergander, *Organometallics* **1998**, *17*, 2183–2187; e) D. J. Parks, W. E. Piers, M. Parvez, R. Atencio, M. Zaworotko, *Organometallics* **1998**, *17*, 1369–1377; f) D. Vagedes, R. Fröhlich, G. Erker, *Angew. Chem.* **1999**, *111*, 3561–3565; *Angew. Chem. Int. Ed.* **1999**, *38*, 3362–3365; g) L. H. Doerrer, M. L. H. Green, *J. Chem. Soc. Dalton Trans.* **1999**, 4325–4329; h) R. E. LaPointe, G. R. Roof, K. A. Abboud, J. Klosin, *J. Am. Chem. Soc.* **2000**, *122*, 9560–9561; i) C. Bergquist, B. M. Bridgewater, C. J. Harlan, J. R. Norton, R. A. Friesner, G. Parkin, *J. Am. Chem. Soc.* **2000**, *122*, 10581–10590; j) R. Duchateau, R. A. Van Santen, P. A. Yap, *Organometallics* **2000**, *19*, 809–816; k) G. Kehr, R. Roesmann, R. Fröhlich, C. Holst, G. Erker, *Eur. J. Inorg. Chem.* **2001**, 535–538; l) J. Zhou, S. J. Lancaster, D. A. Walker, S. Beck, M. Thornton-Pett, M. Bochmann, *J. Am. Chem. Soc.* **2001**, *123*, 223–237; m) S. J. Lancaster, A. Rodriguez, A. Lara-Sanchez, M. D. Hannant, D. A. Walker, D. H. Hughes, M. Bochmann, *Organometallics* **2002**, *21*, 451–453; n) F. Schaper, H.-H. Brintzinger, *Acta Crystallogr. Sect. E* **2002**, *58*, 77–78; o) D. Vagedes, G. Erker, R. Fröhlich, *J. Organomet. Chem.* **2002**, *641*, 148–155; **2002**, 651, 157; p) D. Vagedes, G. Kehr, D. König, K. Wedeking, R. Fröhlich, G. Erker, C. Mück-Lichtenfeld, S. Grimme, *Eur. J. Inorg. Chem.* **2002**, 2015–2021; q) J. M. Blackwell, W. E. Piers, M. Parvez, R. McDonald, *Organometallics* **2002**, *21*, 1400–1407; r) D. Vagedes, G. Erker, G. Kehr, K. Bergander, O. Kataeva, R. Fröhlich, S. Grimme, C. Mück-Lichtenfeld, *Dalton Trans.* **2003**, 1337–1344; s) I. C. Vei, S. I. Pascu, M. L. H. Green, J. C. Green, R. E. Schilling, G. D. W. Anderson, L. H. Rees, *Dalton Trans.* **2003**, 2550–2557; t) S. Guidotti, I. Camurati, F. Focante, L. Angellini, G. Moscardi, L. Resconi, R. Leardini, D. Nanni, P. Mercandelli, A. Sironi, T. Beringhelli, D. Maggioni, *J. Org. Chem.* **2003**, *68*, 5445–5465; u) A. J. Mountford, W. Clegg, R. W. Harrington, S. M. Humphrey, S. J. Lancaster, *Chem. Commun.* **2005**, 2044–2046; v) J. Sanchez-Nieves, L.-M. Frutos, P. Royo, O. Castano, E. Herdtweck, *Organometallics* **2005**, *24*, 2004–2007; w) A. J. Mountford, S. J. Lancaster, S. J. Coles, P. N. Horton, D. L. Hughes, M. B. Hursthouse, E. L. Mark, *Inorg. Chem.* **2005**, *44*, 5921–5933; x) F. Froctane, I. Camurati, L. Resconi, S. Guidotti, T. Beringhelli, G. D'Alfonso, D. Donghi, D. Maggioni, P. Mercandelli, A. Sironi, *Inorg. Chem.* **2006**, *45*, 1683–1692; y) F. Froctane, R. Leardini, A. Mazzanti, P. Mercandelli, D. Nanni, *Organometallics* **2006**, *25*, 2166–2172; z) Review: G. Erker, *Dalton Trans.* **2005**, 1883–1890.

[16] F. H. Allen, O. Kennard, D. G. Watson, L. Brammer, G. Orpen, R. Taylor, *J. Chem. Soc. Perkin Trans.* **1987**, S1–S19.

[17] a) S. Grimme, *J. Comput. Chem.* **2004**, *25*, 1463–1476; b) M. Piacenza, S. Grimme, *ChemPhysChem* **2005**, *6*, 1554–1558; c) M. Piacenza, S. Grimme, *J. Am. Chem. Soc.* **2005**, *127*, 14841–14848; d) M. Parac, M. Etinski, M. Peric, S. Grimme, *J. Chem. Theory Comput.* **2005**, *1*, 1110–1118.

[18] B. Bo Zou, K. Dreger, C. Mück-Lichtenfeld, S. Grimme, H. J. Schäfer, H. Fuchs, L. Chi, *Langmuir* **2005**, *21*, 1364–1370.

[19] J. P. Perdew, K. Burke, M. Ernzerhof, *Phys. Rev. Lett.* **1996**, *77*, 3865–3868.

[20] S. Grimme, *J. Chem. Phys.* **2003**, *118*, 9095–9102.

[21] J. R. Durig, Y. S. Li, L. A. Carreira, J. D. Odom, *J. Am. Chem. Soc.* **1973**, *95*, 2491–2496.

[22] S. S. Mallajosyula, A. Datta, S. K. Pati, *J. Phys. Chem. A* **2006**, *110*, 5156–5163.

[23] A good understanding of the bonding and conformational features of $R_3P{-}BR'_3$ adducts seems essential for the further development of the recently discovered H_2 activation features of some of those systems: a) G. C. Welch, R. R. S. Juan, J. D. Masuda, D. W. Stephan, *Science* **2006**, *314*, 1124–1126; b) G. C. Welch, D. W. Stephan, *J. Am. Chem. Soc.* **2007**, *129*, 1880–1881.

[24] a) V. Jäger, H. G. Viehe, *Methoden Org. Chem. (Houben-Weyl)*, 4th edition **1977**, V/2a, *123*; b) K. B. Starowieyski, A. Chojnowski, Kusmierek, Z. **1980**, *192*, 147–154; c) S. L. Bender, M. R. Detty, N. F. Haley, *Tetrahedron Lett.* **1982**, *23*, 1531–1534.

[25] R. Ahlrichs, M. Bär, M. Häser, H. Horn, C. Kölmel *Chem. Phys. Lett.* **1989**, 162, 165–169; TURBOMOLE (Vers. 5.6): R. Ahlrichs et al, Universität Karlsruhe **2003**. See also: http://www.turbomole.com.

[26] A. Schäfer, C. Huber, R. Ahlrichs, *J. Chem. Phys.* **1994**, *100*, 5829–5835; the basis sets are available from the TURBOMOLE homepage via the FTP Server Button (in the subdirectories basen, jbasen, and cbasen). See http://www.turbomole.com.

[27] a) K. Eichkorn, O. Treutler, H. Öhm, M. Häser, R. Ahlrichs, *Chem. Phys. Lett.* **1995**, *240*, 283–290; b) K. Eichkorn, F. Weigend, O. Treutler, R. Ahlrichs, *Theor. Chem. Acc.* **1997**, 97, 119–124; c) F. Weigend, M. Häser, *Theor. Chem. Acc.* **1997**, 97, 331–340; d) F. Weigend, A. Köhn, C. Hättig, *J. Chem. Phys.* ***2002**, 116, 3175–3183.*

[28] Z. Otwinowski, W. Minor, *Methods Enzymology*, **1997**, *276*, 307–326.

[29] R. H. Blessing, *Acta Crystallogr. Sect. A* **1995**, *51*, 33–37; R. H. Blessing, *J. Appl. Crystallogr.* **1997**, *30*, 421–426.

[30] Z. Otwinowski, D. Borek, W. Majewski, W. Minor, *Acta Crystallogr. Sect. A.* **2003**, *59*, 228–234.

[31] G. M. Sheldrick, *Acta Crystallogr. Sect. A* **1990**, *46*, 467–473.

[32] SHELXL-97, program for crystal structure refinement, G. M. Sheldrick, Universität Göttingen, Göttingen (Germany), **1997**.

[33] E. Keller, Universität Freiburg, Freiburg (Germany), **1997**.

Received: April 27, 2007
Published online: September 25, 2007

